Princeton Plasma Physics Laboratory

PPPL-5322

Measurement of Deuterium Density Profiles in the H-mode Steep Gradient Region Using Charge Exchange Recombination Spectroscopy on DIII-D

S.R. Haskey, B.A. Grierson, N.A. Pablant

August 2016

Prepared for the U.S. Department of Energy under Contract DE-AC02-09CH11466.

Princeton Plasma Physics Laboratory
Report Disclaimers

Full Legal Disclaimer

Trademark Disclaimer

PPPL Report Availability

Princeton Plasma Physics Laboratory:

http://www.pppl.gov/techreports.cfm

Office of Scientific and Technical Information (OSTI):

http://www.osti.gov/scitech/

Related Links:

U.S. Department of Energy

U.S. Department of Energy Office of Science

U.S. Department of Energy Office of Fusion Energy Sciences

Measurement of deuterium density profiles in the H-mode steep gradient region using charge exchange recombination spectroscopy on DIII-D[a)]

S. R. Haskey,[1, b)] B. A. Grierson,[1] K. Burrell,[2] C. Chrystal,[3] R. J. Groebner,[2] D. H. Kaplan,[2] N. A. Pablant,[1] and L. Stagner[4]

[1)] *Princeton Plasma Physics Laboratory, Princeton, New Jersey 08543-0451, USA*
[2)] *General Atomics, PO Box 85608, San Diego, CA 92186, USA*
[3)] *Oak Ridge Associated Universities, Oak Ridge, TN 37831, USA*
[4)] *University of California, Irvine, California 92697, USA*

(Dated: 29 August 2016)

Recent completion of a thirty two channel main-ion (deuterium) charge exchange recombination spectroscopy (CER) diagnostic on the DIII-D tokamak [J. L. Luxon, Nucl. Fusion 42 **614** (2002)] enables detailed comparisons between impurity and main-ion temperature, density, and toroidal rotation. In an H-mode DIII-D discharge these new measurement capabilities are used to provide the deuterium density profile, demonstrate the importance of profile alignment between Thomson scattering and CER diagnostics, and aid in determining the electron temperature at the separatrix. Sixteen sightlines cover the core of the plasma and another sixteen are densely packed towards the plasma edge, providing high resolution measurements across the pedestal and steep gradient region in H-mode plasmas. Extracting useful physical quantities such as deuterium density is challenging due to multiple photoemission processes. These challenges are overcome using a detailed fitting model and by forward modeling the photoemission using the FIDASIM code, which implements a comprehensive collisional radiative model.

The ability to predict and optimize the performance of future magnetic confinement devices such as ITER requires the continued development and validation of sophisticated transport models. Accurate measurements of the main-ion species' properties are required to validate these models through momentum, particle, and energy transport studies. Typically, impurity charge exchange spectroscopy (CER) is used to measure the temperature, velocity, and density of an impurity species, with the main-ion properties either being assumed to be equal, or inferred using neoclassical models. Recent completion of a sixteen channel edge main-ion (deuterium) CER diagnostic[1] on the DIII-D tokamak, which complements an existing core system[2], provides direct measurements of the main-ion properties allowing more accurate transport studies to be performed, and differences in the properties of the deuterium and impurities to be explored. Main-ion CER sightlines share the same optics and are interleaved with sightlines on the recently upgraded impurity CER system[3] allowing straightforward comparisons. The success of the main-ion diagnostic is due primarily to advances in forward modeling the complex photoemission processes, using a sophisticated spectral fitting routine that includes all relevant features in the D_α emission spectrum[4], and separating the active emission from the passive emission using beam modulation and active-passive time slice subtraction.

Section I describes the forward modeling and other important factors which need to be taken into account when interpreting the D_α spectrum in the pedestal. Examples of main-ion measurements in H-mode plasmas including a deuterium density profile are shown in section II. Lastly section III demonstrates how the new measurements can be used to align the Thomson scattering and CER systems in flux co-ordinates.

I. D_α PHOTOEMISSION

The D_α spectrum is substantially more complex than impurity emission, which is typically used for CER spectroscopy. Forward modeling of the D_α emission is performed using the comprehensive collisional radiative model implemented in the recently upgraded FIDASIM code[5,6], which is used from within OMFIT[7]. FIDASIM calculates the density of multiple neutral deuterium populations (thermal, beam, fast) in several principle quantum states on a simulation grid, as well as the associated photoemission using the following inputs: beam parameters, viewing geometry, EFIT equilibrium[8], electron density and temperature (n_e, T_e), ion temperature and angular rotation (T_i, Ω_i), and an impurity and main-ion density (n_D).

A FIDASIM output of particular interest for this work is the density of deuterium in the $n = 3$ excited state (Fig. 1) which are responsible for D_α emission via the $n = 3 \rightarrow 2$ transition (6561Å) with Doppler broadening and shifts dependent on the properties of the respective emitting populations. There are several distinct neutral populations including injected beam neutrals with full [Fig. 1 (a)], half and third energies, fast neutrals, and thermal neutrals [Fig. 1 (b)]. The thermal neutrals (n_t) can be split into two sub-populations depending on the species that donated the electron in the charge exchange

[a)] Contributed paper published as part of the Proceedings of the 21st Topical Conference on High-Temperature Plasma Diagnostics (HTPD 2016) in Madison, Wisconsin, USA.
[b)] Electronic mail: shaskey@pppl.gov

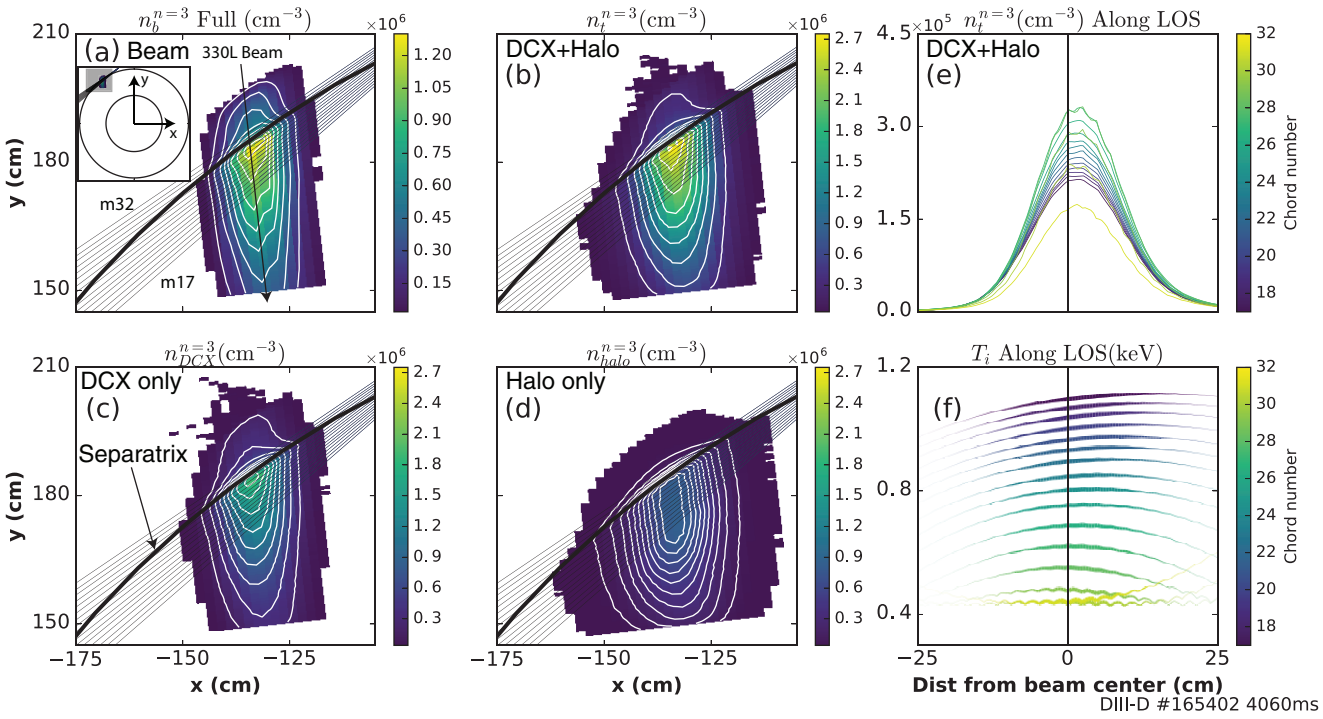

FIG. 1. Midplane view of the FIDASIM forward modeled excited ($n = 3$) neutral deuterium density due to several different populations. Thick black curve is the plasma edge and thin lines are the main-ion diagnostic sightlines. The shaded square on the inset plot in (a) provides orientation for the other plots. Full energy beam neutral population (a), direct charge exchange neutrals (c), halo neutrals (d), and total thermal neutrals (DCX + halo) (b). The 16 edge chord sightlines are shown along with the $n = 3$ density (e) and variation in ion temperature (f) along the sightlines [see (a) for chord numbers], x-axis is distance along the LOS to the beam center. The line thickness in (f) represents the $n = 3$ neutral density [from (b)] normalized to the maximum value along the LOS to show the signal weighting.

reaction. Those that are born through charge exchange with a beam neutral are termed direct charge exchange (DCX) neutrals, and may be considered the first generation of thermal neutrals [Fig. 1 (c)]. The donor can also be a thermal neutral, in which case the born thermal neutrals are referred to as halo neutrals and may be regarded as 2nd generation or higher [Fig. 1 (d)].

Due to differences in their D_α emission, it is useful to consider the DCX neutrals and halo neutrals separately. DCX emission suffers from cross-section distortions while halo emission suffers from line of sight integration effects because it is more diffuse[2] [compare Fig. 1 (b) and (c)]. Plotting the density of thermal neutrals in the $n = 3$ state along the measurement lines of sight (LOS) clearly shows that these measurements have finite LOS integration effects [Fig. 1 (e) and (f)]. Fig. 2 shows the DCX and halo contributions to the thermal feature in the D_α spectrum, calculated using FIDASIM. They have slightly different Doppler shifts and are often of comparable amplitude. In the measured spectrum, due to their similarity, it is not possible to fit these features separately and correct for them individually. However, fitting the overall spectrum from FIDASIM gives an apparent temperature, velocity, and brightness, which are used to calculate a correction to raw tokamak data (deuterium density, temperature, and toroidal velocity) through an iterative process. Currently FIDASIM iterations are performed for each time slice because the sharp profile gradients at the plasma edge complicate the lookup table approach that was previously used for the core main-ion CER system on DIII-D[2].

II. MAIN-ION DENSITY, TEMPERATURE, AND ROTATION PROFILES

A DIII-D ITER baseline scenario (#165402) is investigated because the steep electron density pedestal provides a good test for the edge main-ion diagnostic. Kinetic profiles for the e, C^{+6}, and D^+ are shown in Fig. 3 using a magnetics only EFIT. For the deuterium temperature and rotation, the apparent measured values are shown. To calculate the corrected values, an iterative process is required where the actual deuterium profiles (initially guesses) are input to FIDASIM. FIDASIM outputs the apparent values which are compared with the apparent measurements to create a residual which is used to update the input profiles. This process is iterated until

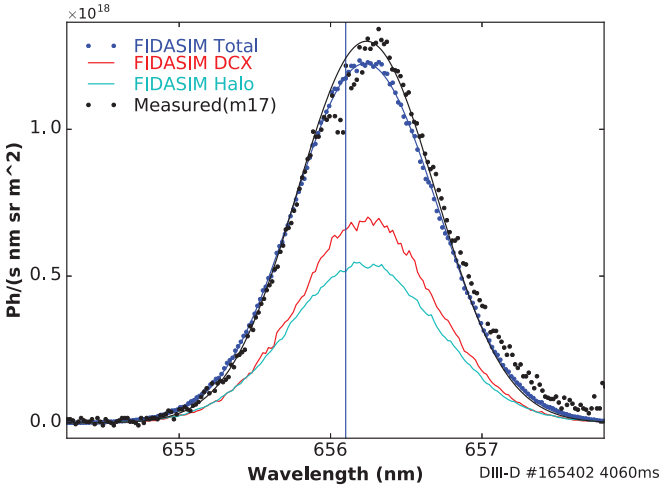

FIG. 2. Excellent agreement between the forward modeled spectrum from FIDASIM and the experimental measurements for the innermost edge chord [see Fig. 1 (a) for chord location]. The FIDASIM modeled contributions to the spectrum due to DCX and halo emission are also shown.

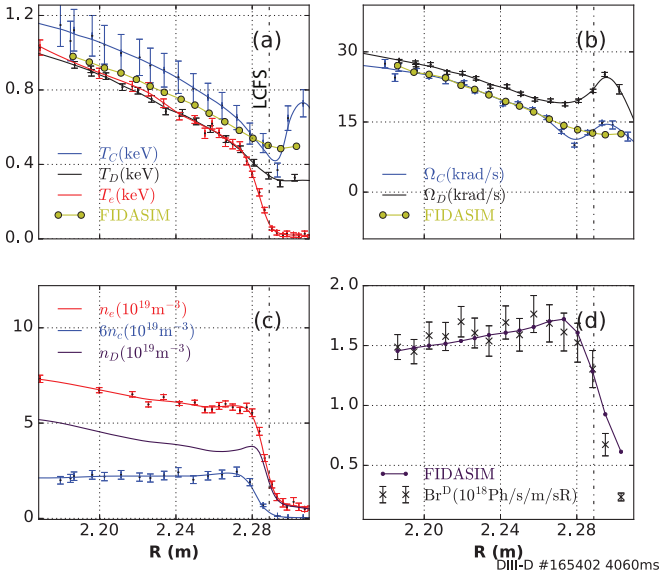

FIG. 3. Comparisons between the temperature (a), rotation (b), and density (c) profiles for the various species. The deuterium profiles are apparent values from fits to experimental data as in Fig. 2. T_C and Ω_C were used as the inputs for the first FIDASIM iteration, with the output apparent values also shown.

agreement is found between the FIDASIM outputs and the apparent measurements meaning the input deuterium profiles will produce the apparent measurements. Details of this procedure and comparisons between impurity and main-ion rotation and temperature will be described in a future publication. To start the iteration procedure the FIDASIM inputs are set to the carbon measurements.

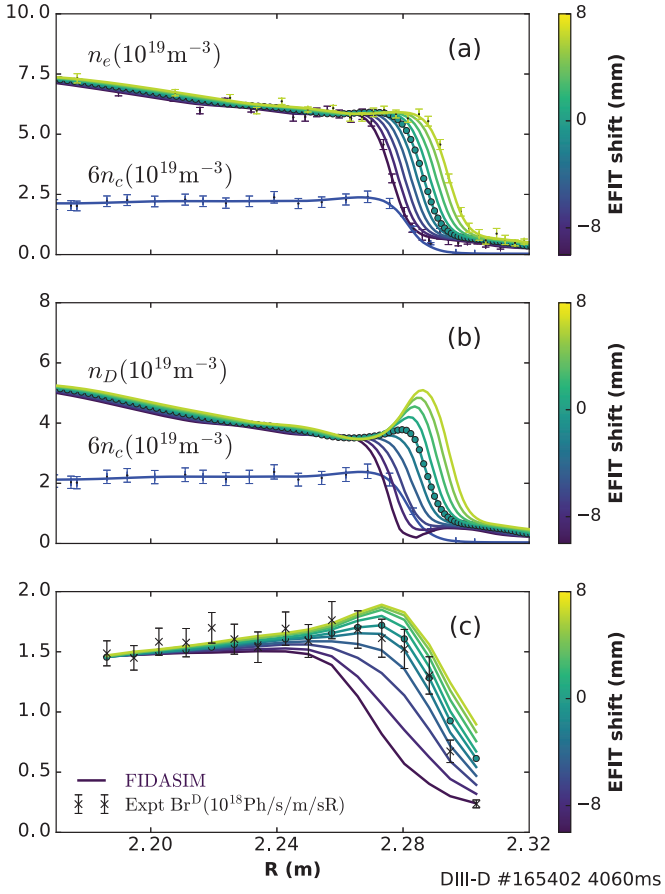

FIG. 4. Effects of shifting the EFIT equilibrium radially with TS profiles fixed in flux co-ordinates and CER profiles fixed in real-space. The circles represent the case where there is no radial shift. The relative shift causes large variations in n_D calculated using quasi-neutrality (b). (c) These different profiles cause large differences in the forward modeled brightness from FIDASIM, with the best agreement with experiment coming from the case with no radial shift.

The FIDASIM apparent output values after this first iteration are shown in Fig. 3. The next iteration would modify the FIDASIM input profiles using the difference between the apparent FIDASIM outputs and apparent measured values. Here, the process is not iterated to completion, but based on the results from the first step, the corrections would make T_D slightly lower but within the error bars of T_C. Almost no correction would be required for Ω_D (black), which shows significantly faster rotation and a non-monotonic feature at the plasma edge compared with carbon (blue). One of the major goals of the main-ion system is to compare impurity and main-ion rotation at the plasma edge and provide critical measurements for intrinsic rotation studies.

The deuterium ion density profile is usually calculated using n_e and the dominant impurity density [C^{6+} (n_c) on DIII-D] through quasi-neutrality. On DIII-D the Thomson scattering (TS) measurements[9] are located vertically

and at a different toroidal location than the magnetics[10] and tangential midplane edge CER measurements, which are in the same sector. Consequently, the n_D profile calculation requires an EFIT[8] equilibrium to map the n_e measurements to the CER chord locations in flux coordinates, which are assumed to be correct. Mapping errors in this process can lead to large variation in the inferred n_D and, more strongly, ∇n_D in the steep gradient region. Fundamentally, the mis-alignment error occurs because the EFIT reconstruction assumes that the plasma is axisymmetric whereas the equilibrium is really 3D due to various error fields, toroidal field ripple, applied 3D fields[11], etc. To compensate for this, the additional constraint that T_e is $\approx$ 80eV at the separatrix[12] is often added to the EFIT, effectively shifting the TS profiles relative to the CER profiles. The brightness of the thermal D_α emission measured by the main-ion CER chords provides a new technique for validating the profile alignment and this T_e constraint (Section III).

There is excellent agreement between the measured and forward modeled brightness from FIDASIM (Fig. 3 (d)) based on the input density profiles in Fig. 3 (c). This demonstrates the ability of the main-ion system to provide a deuterium density profile directly. In this case the initial deuterium density profile guess (based on quasineutrality) agrees with the brightness measurements. In other situations several more iterations may be required. The over prediction of the main-ion brightness outside the last closed flux surface is likely due to an under-estimation of the carbon density due to contributions from lower charge states of carbon, which become significant at lower temperatures and are not measured or included in the quasi-neutrality calculation. The ability to provide a deuterium density measurement directly is particularly valuable in situations where measurements of a significant impurity are not available.

III. ALIGNMENT BETWEEN THOMSON SCATTERING AND CER SYSTEMS

To test the sensitivity to mis-alignment, a scan is performed by fixing the electron density profile in flux coordinates and fixing the CER profiles in real-space. The equilibrium is then shifted radially by $\pm$8mm. This changes the alignment between the TS and CER. As can be seen in Fig. 4 (a) and (b), the shift in n_e (in real-space) leads to large variations in the n_D (from quasi-neutrality) profile, causing either a peak at the top of the pedestal or a trough at the bottom of the pedestal. For each of these cases, the main-ion brightness was forward modeled using FIDASIM and compared with the experimental values [Fig. 4 (c)]. The forward modeled profile changes significantly demonstrating that the diagnostic should be capable of capturing these differences in the n_D pedestal. It is also clear that a shift of $<$ 1mm (marked with circles and also shown in Fig. 3) is optimal for this case where the EFIT has been constrained so that T_e(sep) = 80eV. We also note that for the optimal case, the n_D profile is shifted outwards compared with n_C and there is neither a trough at the bottom of the pedestal, nor a peak at the top. If the scan is repeated for the case where the T_e(sep) = 80eV constraint is not included, there is significant disagreement between the measured brightness and forward modeled brightness. To bring them into agreement a large $\approx$ 1cm radial shift of the equilibrium is required. This highlights the existence of an alignment issue, the ability of the new main-ion diagnostic to resolve the alignment issue, and shows that the T_e(sep) = 80eV constraint can provide a good approximation for the required alignment between TS and CER on DIII-D.

IV. ACKNOWLEDGMENTS

This work supported in part by the U.S. Department of Energy under DE-AC02-09CH11466. The author gratefully acknowledges useful discussions with A. Bortolon, W. W. Heidbrink, N. Logan, O. Meneghini, R. Nazikian, and S. Smith.

[1] B. A. Grierson, K. H. Burrell, C. Chrystal, R. J. Groebner, S. R. Haskey, and D. H. Kaplan, Review of Scientific Instruments (accepted) HTPD , 1 (2016).
[2] B. A. Grierson, K. H. Burrell, C. Chrystal, R. J. Groebner, D. H. Kaplan, W. W. Heidbrink, J. M. Mu??oz Burgos, N. A. Pablant, W. M. Solomon, and M. A. Van Zeeland, Review of Scientific Instruments **83**, 10D529(6) (2012).
[3] C. Chrystal, K. H. Burrell, B. A. Grierson, S. R. Haskey, R. J. Groebner, D. H. Kaplan, and A. Briesemeister, Review of Scientific Instruments **87**, 11E512 (2016).
[4] N. A. Pablant, K. H. Burrell, R. J. Groebner, C. T. Holcomb, and D. H. Kaplan, Review of Scientific Instruments **81**, 10D729 (2010).
[5] W. W. Heidbrink, D. Liu, Y. Luo, E. Ruskov, and B. Geiger, Communications in Computational Physics **10**, 716 (2011).
[6] L. Stagner, "FIDASIM code repository, https://github.com/D3DEnergetic/FIDASIM," (2016).
[7] O. Meneghini, S. Smith, L. Lao, O. Izacard, Q. Ren, J. Park, J. Candy, Z. Wang, C. Luna, V. Izzo, B. Grierson, P. Snyder, C. Holland, J. Penna, G. Lu, P. Raum, A. McCubbin, D. Orlov, E. Belli, N. Ferraro, R. Prater, T. Osborne, A. Turnbull, and G. Staebler, Nuclear Fusion **55**, 083008 (2015).
[8] L. Lao, H. St. John, R. Stambaugh, A. Kellman, and W. Pfeiffer, Nuclear Fusion **25**, 1611 (1985).
[9] D. Eldon, B. D. Bray, T. M. Deterly, C. Liu, M. Watkins, R. J. Groebner, A. W. Leonard, T. H. Osborne, P. B. Snyder, R. L. Boivin, and G. R. Tynan, Review of Scientific Instruments **83**, 10E343 (2012).
[10] J. D. King, E. J. Strait, R. L. Boivin, D. Taussig, M. G. Watkins, J. M. Hanson, N. C. Logan, C. Paz-Soldan, D. C. Pace, D. Shiraki, M. J. Lanctot, R. J. La Haye, L. L. Lao, D. J. Battaglia, A. C. Sontag, S. R. Haskey, and J. G. Bak, Review of Scientific Instruments **85**, 083503 (2014).
[11] S. R. Haskey, M. J. Lanctot, Y. Q. Liu, J. M. Hanson, B. D. Blackwell, and R. Nazikian, Plasma Physics and Controlled Fusion **56**, 35005 (2014).
[12] P. Ghendrih, *Plasma Physics and Controlled Fusion*, Vol. 43 (Institute of Physics Publishing Bristol, 2001) pp. 223–224.

PPPL PRINCETON PLASMA PHYSICS LABORATORY

Princeton Plasma Physics Laboratory
Office of Reports and Publications

Managed by
Princeton University

under contract with the
U.S. Department of Energy
(DE-AC02-09CH11466)

P.O. Box 451, Princeton, NJ 08543
Phone: 609-243-2245
Fax: 609-243-2751

E-mail: publications@pppl.gov

Website: http://www.pppl.gov